Integration of patient specific modeling and advanced image processing techniques for image guided neurosurgery

[1] Neculai Archip, [2] Andriy Fedorov, [1] Bryn Lloyd, [2] Nikos Chrisochoides, [3] Alexandra Golby, [3] Peter M. Black, [1] Simon K. Warfield

[1] Computational Radiology Laboratory, Harvard Medical School, Children's Hospital, [3] Brigham and Women's Hospital, Boston, MA, USA

[2] Computer Science Department, College of William and Mary, Williamsburg, VA, USA

ABSTRACT

A major challenge in neurosurgery oncology is to achieve maximal tumor removal while avoiding postoperative neurological deficits. Therefore, estimation of the brain deformation during the image guided tumor resection process is necessary.

While anatomic MRI is highly sensitive for intracranial pathology, its specificity is limited. Different pathologies may have a very similar appearance on anatomic MRI. Moreover, since fMRI and diffusion tensor imaging are not currently available during the surgery, non-rigid registration of preoperative MR with intra-operative MR is necessary.

This article presents a translational research effort that aims to integrate a number of state-of-the-art technologies for MRI-guided neurosurgery at the Brigham and Women's Hospital (BWH). Our ultimate goal is to routinely provide the neurosurgeons with accurate information about brain deformation during the surgery.

The current system is tested during the weekly neurosurgeries in the open magnet at the BWH. The pre-operative data is processed, prior to the surgery, while both rigid and non-rigid registration algorithms are run in the vicinity of the operating room.

The system is tested on 9 image datasets from 3 neurosurgery cases. A method based on edge detection is used to quantitatively validate the results. 95% Hausdorff distance between points of the edges is used to estimate the accuracy of the registration.

Overall, the minimum error is 1.4 mm, the mean error 2.23 mm, and the maximum error 3.1 mm. The mean ratio between brain deformation estimation and rigid alignment is 2.07. It demonstrates that our results can be 2.07 times more precise then the current technology.

The major contribution of the presented work is the rigid and non-rigid alignment of the pre-operative fMRI with intra-operative 0.5T MRI achieved during the neurosurgery.

Keywords: image guided neurosurgery, rigid registration, non-rigid registration, brain deformation, mesh generation

1. INTRODUCTION

Key surgical challenges for neurosurgeons during tumor resection are to (1) remove as much tumor tissue as possible, (2) minimize the removal of healthy tissue (3) avoid the disruption of critical anatomical structures, and (4) know when to stop the resection process. The development of intra-operative imaging systems has contributed to improving the course of intra-cranial neurosurgical procedures. Among these systems, the

0.5T intraoperative magnetic resonance scanner of the Brigham and Women's Hospital (BWH), Boston, offers the possibility to acquire 256 x 256 x 58 (0.86 mm, 0.86 mm, 2.5 mm) T1 weighted images with the fast spin echo protocol (TR = 400, TE = 16 ms, FOV = 220x220 mm) in 3 minutes and 40 seconds. The intra-operative MR scanner enhances the surgeon's view and enables the visualization of the brain deformation during the procedure. The location of both the tumor, as well as other critical structures that need to be preserved, may shift from their pre-operative locations due to these deformations, significantly diminishing the accuracy of the neuro-navigation procedure planned pre-operatively.
The time constraint on this overall procedure is severe since all the steps starting from intra-operative image acquisition to final visualization need to happen within ~20 minutes to be of practical use to the neurosurgeons. Current prototype system at BWH uses a homogeneous, linear elastic material model of the brain for the biomechanical simulation, since only this crude and less accurate model is able to meet the real time constraint of IGNS on the available onsite compute power at the BWH hospital. The crude biomechanical model based image update is provided to the neurosurgeons throughout the six or eight hours long surgical process at a constant rate of approximately once an hour. The current prototype system is shown in Figure 1.

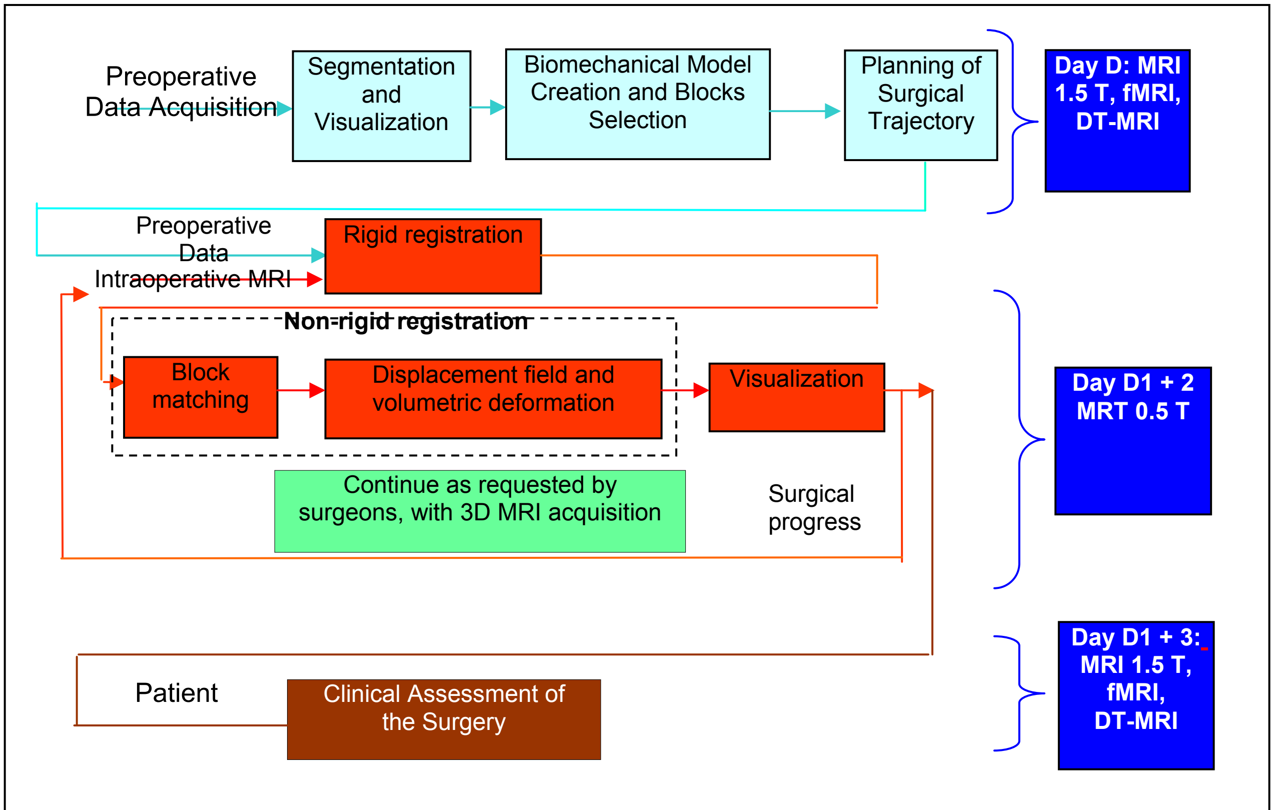

Figure 1. The current system for the image guided neurosurgery

Early in the surgery, once the tumor is identified, the procedure involves removing the middle of the tumor and working out towards the edges. A great deal of brain deformation can occur as the main mass of the tumor is debulked and the brain shifts as it can be seen in the Figure 2. During this stage of the surgery, the surgeon may only wish to acquire new images once per hour. However, towards the end of the procedure, the surgeon approaches the edge of the tumor, taking away smaller and smaller amounts of tumor and trying hard to guess where to stop the resection process.

(a) **(b)**

Figure 2. Two Dimensional View of Brain Shift. (a) Pre-operative Image. (b) Intra-operative Image (after the dura has been open and part of the tumor removed).

In this article we report our efforts to integrate a number of state-of-the-art technologies for MRI-guided neurosurgery at the Brigham and Women's Hospital (BWH), Boston. These include advanced intra-operative imaging, image registration and visualization for fusing multiple modalities while accounting for "brain shift", in order to identify and differentiate pathologies from healthy tissue throughout the course of a surgical procedure, as well as to evaluate its outcome. The main challenge is to bring these technologies to be routinely used in a clinical setting. We describe results of the overall accuracy of our system, obtained during neurosurgery cases at BWH. Non-rigid alignment of pre-operative fMRI and intra-operative T1 is also demonstrated.

2. METHODS

The system uses patient specific models to quantify the brain deformation. The algorithm can be decomposed into three main parts. The first part consists in building the patient-specific model utilizing intra-operative MRI. The second part is the block matching computation for selected blocks which estimates a set of displacements across the volume. The third part is an iterative hybrid solver that estimates the 3D volumetric deformation field, utilizing the anisotropic information provided by the structure tensor computed for each block. Details can be found in [1].

In the planning phase, the brain segmentation is performed, followed by biomechanical modeling. During the neurosurgery, the pre-operative data (3T) is rigidly aligned with the first intra-operative scan (0.5T). Non-rigid registration is applied to the subsequent MR scans. The data is transferred during the intervention and processed in the vicinity of the OR.

The main components of the system are:

2.1. Image segmentation: The delineation of structures in the preoperative data is achieved using segmentation strategies optimized for the particular type of acquisition [2]. This approach combines the benefits of anatomical information, statistical classification and elastic matching to achieve results superior to those which can be obtained by any single method alone. Recently we have also successfully used a method based on deformable model which evolves to fit the brain's surface by the application of a set of locally adaptive model forces [3].

2.2. Mesh generation: Tetrahedral discretization (volume mesh) of the segmented intra-cranial cavity serves as the basis for Finite Element Method (FEM) modeling of the physical tissue deformation, and serves as the function of regularization on the estimated displacements obtained as the result of block matching step of non-rigid registration. The technique we use for tetrahedral mesh generation has been described in [4, 5].

Our implementation of the mesh generation procedure is based on the technique originally described in [6, 7]. It is a heuristic, which is using implicit representation of the object as input, and produces an adaptive

tetrahedral mesh specifically suited for applications which exhibit high deformation. The algorithm operates on the signed distance map of the input object (in our case, signed distance map of the segmented intra-cranial cavity). and does not require explicit or parametric surface description. The quality of the final mesh is not guaranteed, however we had satisfactory quality of the meshes for all of the registration cases completed in the course of the study. An example of mesh is presented in the Figure 3.
The issue of mesh quality evaluation requires additional attention. Thus, we chose to use the following two quality metrics: aspect ratio (ideal value is 1), and minimum dihedral angle (ideal value is around 40^o and should be far from 0^o and less than 90^o) of the element.
The aspect ratio values we observed for the meshes used in this study are in the range between 1.0 and 18.6, and dihedral angles between 6.9^o and 80.7^o.

We evaluate the quality of surface approximation by computing one-way Hausdorff distance between the surface extracted from the segmentations with the Marching cubes algorithm [8] and the mesh surfaces we generate [9]. The mean value of the distance is below 1mm. Illustration 2 shows the color coded the Hausdorff distances for one of the retrospective cases used in [1]; we compared quality approximation metric for a mesh generated with Yams/GHS3D commercial software as described in [1], and the surface of a mesh we generated for the same input. The values of Hausdorff distance for our meshes are comparable with those for the Yams/GHS3D approach. This aspect is illustrated in the Figure 4.

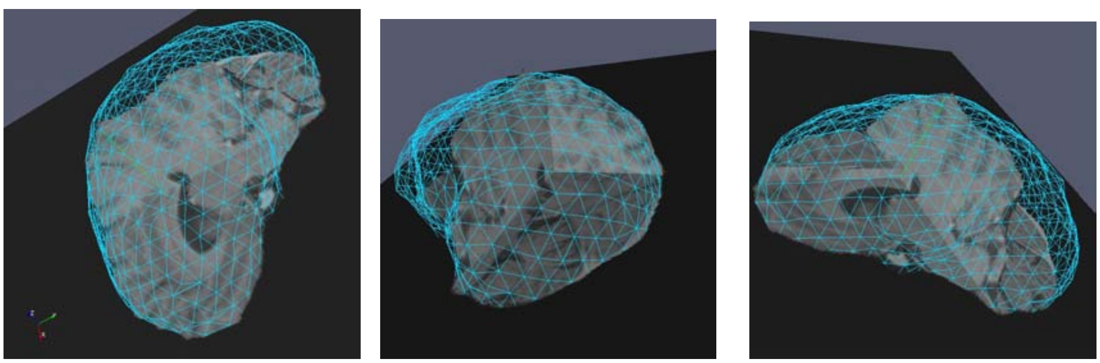

Figure 3: A tetrahedral mesh model of the brain together with the original brain segmentation from the 3T pre-operative MRI.

The described mesh generation approach has been implemented as a collection of ITK classes. It is freely available within the NAMIC SandBox [10].

2.3. Biomechanical model: We model the brain material using an incompressible linear elastic constitutive equation to characterize the mechanical behavior of the brain parenchyma. Because the ventricles and subarachnoid space are connected, the CSF is free to flow from one to another. We thus assume very soft and compressible tissue for the ventricles. The skull is implicitly modeled by preventing the brain mesh vertices to move outside the brain segmentation.
2.4. Rigid registration: A scheme based on Normalized correlation metric is used in an initial phase to align the preop- and first intra-op dataset. The rigid alignment is further refined based on Mattes mutual information metric. The rigid registration algorithms are also based on the ITK library.

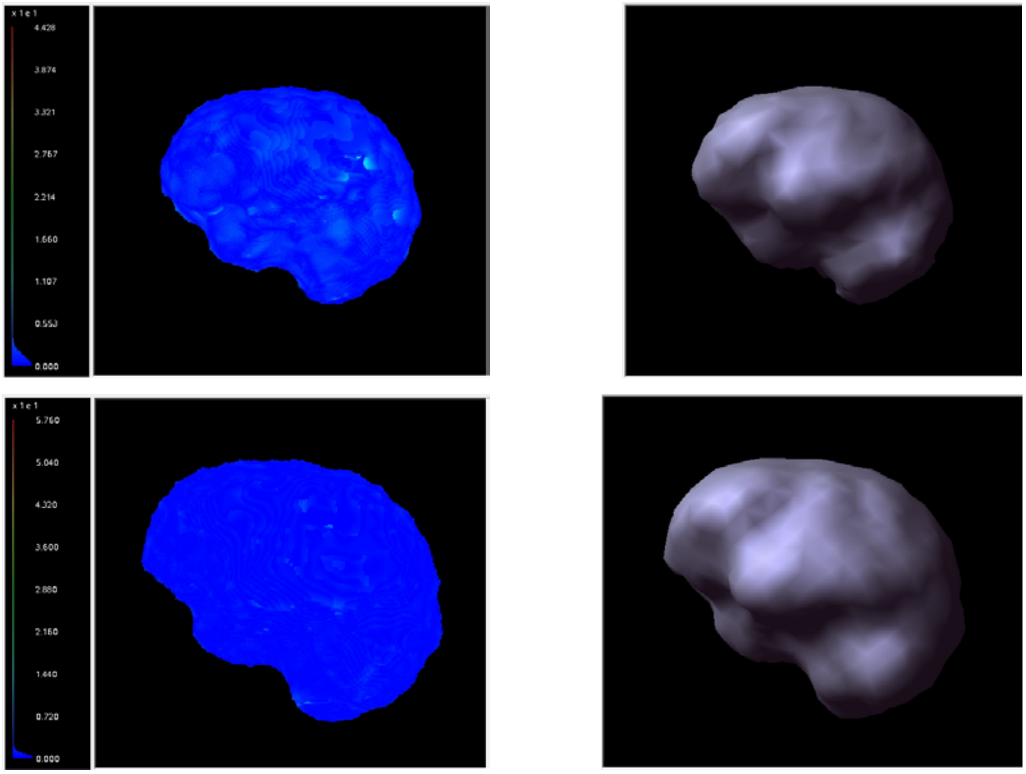

Figure 4. One-sided Hausdorff distance between the Marching cubes surface and a) Yams/GHS3D geenrated mesh surface; b) surface of the mesh generated with the implementation we used.

2.5. Non-rigid registration: The algorithm proposed by our group is used [1]. It relies on a robust estimation of the deformation from a sparse noisy set of measured displacements. The displacement field thus estimated is applied to the fMRI data.

3. RESULTS

The system is evaluated on 9 image datasets from 3 neurosurgery cases. The data is transferred and processed during the neurosurgery. Alignment results are presented in the Figure 5 and 6.

The overall accuracy of the brain deformation quantification is estimated based on the edges extracted from the images. 95% Hausdorff distance is computed between (1) the deformed registered image, and the intra-operative image, and (2) the preoperative data rigid aligned with the intra-operative image. The ideal case is when the distance in (1) is 0.

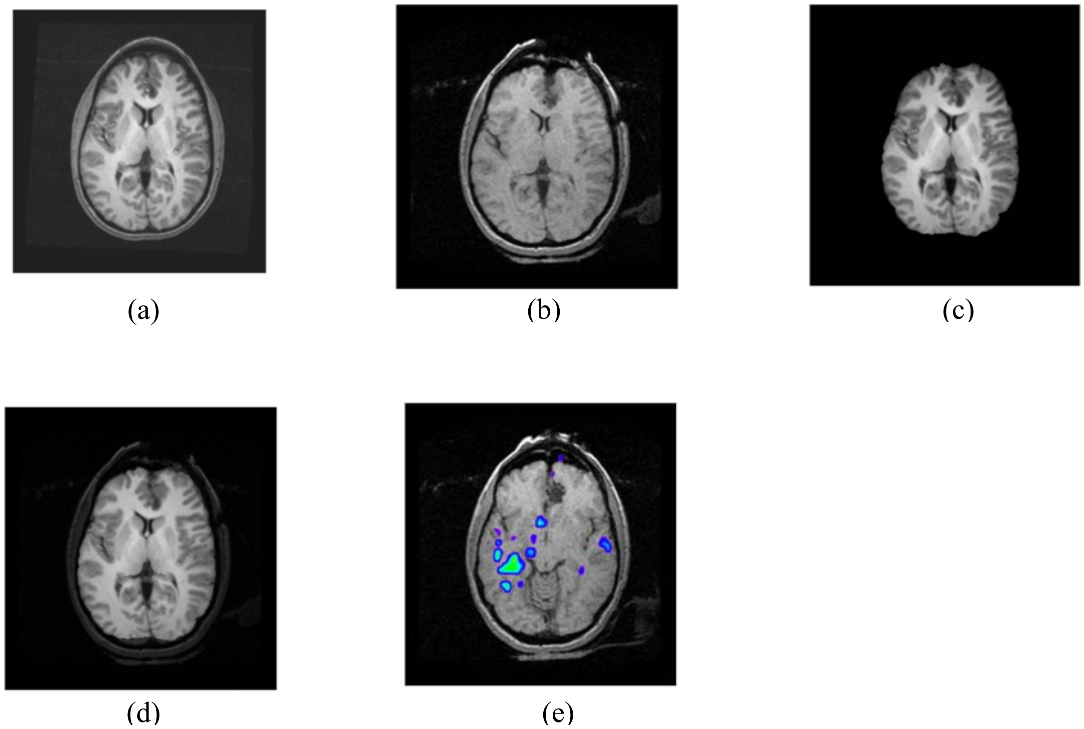

Figure 5. Non-rigid registration results during the neurosurgery between the pre-operative 3T data and intra-operative 0.5T. (a) Pre-operative 3T MRI data; (b) intra-operative scan, 0.5T. (c) Pre-operative brain non-rigid deformed to match an intra-operative scan. (d) the image (c) superimposed on the image (b). Thus the intra-operative scan is enhanced with pre-operative information. (e) The fMRI is also non-rigid aligned with the intra-operative scan.

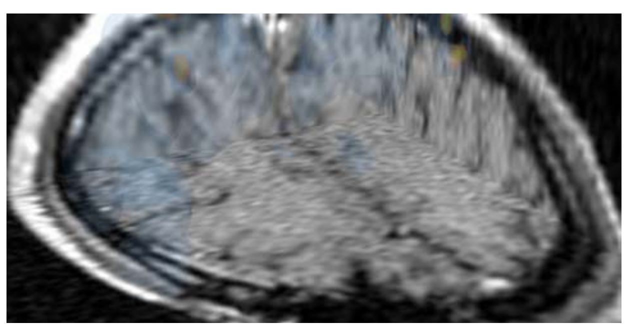

The (2) is used as a comparison, since in the current clinical procedures only rigid registration is performed. We also compute the ratio between the (1) and (2). The 95% Haussdorf ensures that the outliers are rejected. Oerall, the minimum distance obtained is 1.4 mm, the mean 2.23 mm, and the max 3.1 mm. The mean ratio between (2) and (1) is 2.07, that basically states that our results can be 2.07 times more precise then current technology. The complete results are presented in the Table 1. A typical plot of the 95% Hausdorff distance between edges used to validate the algorithms, is presented in the Figure 7.

Dataset #	Non Rigid 95% Haus. (mm)	Rigid 95% Haus. (mm)	Ratio Rigid/Non-Rigid
1	1.7	4.1	2.41
2	1.9	3.0	1.57
3	1.4	4.0	2.85
4	2.9	4.9	1.68
5	2.3	4.2	1.82
6	2.1	4.3	2.04
7	3.1	5.9	1.9
8	2.5	5.3	2.12
9	2.2	5.1	2.31

Table 1. Accuracy measured for rigid and non-rigid registration algorithms.

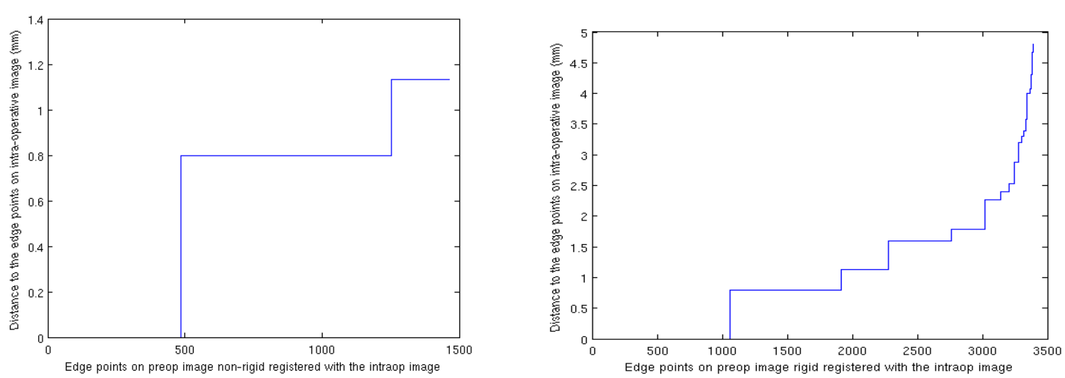

Figure 7. First plot shows the 95% Hausdorff distance between the points on the edges of the registered image and intra-operative image. The second plot presents the 95% Hausdorff between points on the edges on the rigid aligned preoperative image and the edges on the intra-operative data. The number of points on the extracted edges is different in the two cases, since typically MR 1.5 T images have higher contrast.

4. CONCLUSIONS

We have presented a comprehensive framework for computer-integrated surgery that promises to ameliorate some of the clinical difficulties experienced in contemporary image-guided neurosurgery.
We achieved during the neurosurgery rigid and non-rigid registration of (1) pre-operative with intra-operative T1 images; and (2) pre-operative fMRI with intra-operative T1 images.
The system is validated on prospective data acquired at BWH, and results show that the brain deformations are accurately computed.

5. ACKNOWLEDGEMENT

This investigation was supported by NSF ITR 0426558, a research grant from the Whitaker Foundation, a research grant from CIMIT, by NIH grants R21 MH67054, R01 LM007861, P41 RR13218, U41-RR019703.

REFERENCES

[1] O. Clatz, H. Delingette, I.-. Talos, A.J. Golby, R. Kikinis, F.A. Jolesz, N. Ayache and S.K. Warfield, *Robust Non-Rigid Registration to Capture Brain Shift from Intra-Operative MRI*, IEEE Transactions on Medical Imaging, vol. 24, pp. 1417-1427, 2005.
[2] Simon Warfield, Joachim Dengler, Joachim Zaers, Charles R.G. Guttmann, William M. Wells III, Gil J. Ettinger, John Hiller and Ron Kikinis. *Automatic Identification of Grey Matter Structures from MRI to Improve the Segmentation of White Matter Lesions.* The Journal of Image Guided Surgery, volume 1, number 6, 1995, pages 326-338.
[3] S.M. Smith. *Fast robust automated brain extraction.* Human Brain Mapping, 17(3):143-155, November 2002.
[4] A. Fedorov, N. Chrisochoides, R. Kikinis and S.K. Warfield, *Tetrahedral mesh generation for medical imaging*, Insight Journal, vol. 2, pp. January 8, 2006, 2005.
[5] A. Fedorov, N. Chrisochoides, R. Kikinis and S.K. Warfield, *An evaluation of three approaches to tetrahedral mesh generation for deformable registration of MR images*, in Proceedings of IEEE International Symposium on Biomedical Imaging: From Nano to Macro (ISBI 2006), 2006.
[6] R. Bridson, Computational aspects of dynamic surfaces, 2003.
[7] N.P. Molino, R. Bridson, J. Teran and R. Fedkiw, A Crystalline, Red Green Strategy for Meshing Highly Deformable Objects with Tetrahedra, in Proceedings of the 12th International Meshing Roundtable, pp. 103-114, 2003.
[8] W.E. Lorensen and H.E. Cline, *Marching cubes: A high resolution 3D surface construction algorithm*, in Proceedings of the 14th annual conference on Computer graphics and interactive techniques SIGGRAPH'87, pp. 163-169, 1987.
[9] N. Aspert, D. Santa-Cruz and T. Ebrahimi, *MESH: Measuring Error between Surfaces using the Hausdorff distance*, in Proceedings of the IEEE International Conference on Multimedia and Expo 2002 (ICME), pp. 705-708, 2002.
[10] Anonymous *NAMIC SandBox repository page*, vol. 2006, pp. 1, 2006.